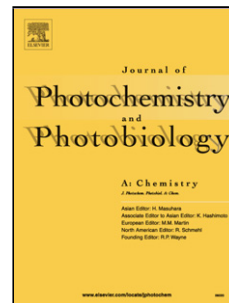


Accepted Manuscript

Title: Role of Cyano Substituents on Thiophene vinylene benzothiadiazole conjugated polymers and application as hole transporting materials in perovskite solar cells

Authors: K. Mahesh, S. Karpagam, Thitirat Putnin, Huong Le, Thanh-Tuân Bui, Kontad Ounnunkad, Fabrice Goubard



PII: S1010-6030(18)30826-8
DOI: <https://doi.org/10.1016/j.jphotochem.2018.11.024>
Reference: JPC 11596

To appear in: *Journal of Photochemistry and Photobiology A: Chemistry*

Received date: 12 June 2018
Revised date: 14 November 2018
Accepted date: 16 November 2018

Please cite this article as: Mahesh K, Karpagam S, Putnin T, Le H, Bui T-Tuân, Ounnunkad K, Goubard F, Role of Cyano Substituents on Thiophene vinylene benzothiadiazole conjugated polymers and application as hole transporting materials in perovskite solar cells, *Journal of Photochemistry and Photobiology, A: Chemistry* (2018), <https://doi.org/10.1016/j.jphotochem.2018.11.024>

This is a PDF file of an unedited manuscript that has been accepted for publication. As a service to our customers we are providing this early version of the manuscript. The manuscript will undergo copyediting, typesetting, and review of the resulting proof before it is published in its final form. Please note that during the production process errors may be discovered which could affect the content, and all legal disclaimers that apply to the journal pertain.

Role of Cyano Substituents on Thiophene vinylene benzothiadiazole conjugated polymers and application as hole transporting materials in perovskite solar cells

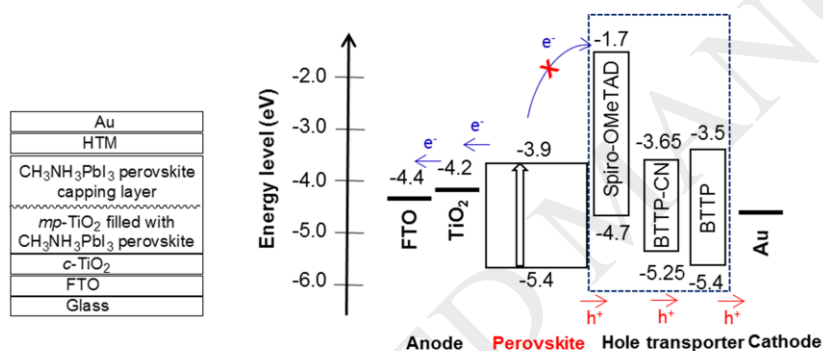
K. Mahesh^a, S. Karpagam^{a*}, Thitirat Putnin^b, Huong Le^c, Thanh-Tuân Bui^c, Kontad Ounnunkad^b, Fabrice Goubard^c

^aDepartment of Chemistry, School of Advanced Sciences, VIT University, Vellore-14, TamilNadu, India. *skarpagam80@yahoo.com

^bDepartment of Chemistry and Center of Excellence for Innovation in Chemistry (PERCH-CIC), Faculty of Science, Chiang Mai University, Chiang Mai 50200, Thailand

^cLaboratoire de Physicochimie des Polymères et des Interfaces, Université de Cergy-Pontoise, 5 mail Gay Lussac, 95031 Neuville-sur-Oise, France

Graphical abstract



Highlights:

- Excellent photoelectronic property of new conjugated polymer contains Thiophene and benzothiadiazole was synthesized
- Excellent orange and yellow fluorescence, low band gap(1.9, 1.6) and good thermal stability of the conjugated polymer
- Great potential to act as Hole transporting materials in Perovskite Solar cells.

ABSTRACT

Two narrow-band gap of donor-acceptor based conjugated polymers, BTTP and BTTP-CN were synthesized by Wittig copolymerization with thiophene or cyano-vinylene thiophene as the donor and 2,1,3-benzothiadiazole as acceptor units. The polymers were investigated by FT-IR, UV-Vis, fluorescence spectroscopy, thermal stability and cyclic voltammetry (CV). The thermal analysis revealed that the BTTP polymer was stable up to 220 °C and BTTP-CN was stable up to 254 °C. The absorption spectra showed absorption maxima at 403 nm for BTTP and 397 nm for BTTP-CN. The polymers BTTP exhibited orange color fluorescence emission at 585 nm and BTTP-CN exhibited yellow color fluorescence emission at 520 nm. The optical band gap values of undoped polymers BTTP and BTTP-CN were calculated as 2.2 and 2.13 eV respectively. Novel synthesized polymers were then enforced as dopant/additive-free hole transport materials in perovskite solar cells. Both polymers has shown the photovoltaic performance of 3.80 % for BTTP and 3.48 % for BTTP-CN under 1 sun illumination. The photovoltaic performance are compared with reference hole transporting material of spiro-OMeTAD with and without additive as 12.53 and 7.55% respectively.

Keywords: Thiophene; 2,1,3-benzothiadiazole; Perovskite solar cell; low band gap; Hole transporting materials;

1. Introduction

Conjugated polymers have drawn significant attention from last two decades for variety of optoelectronic [1] applications such as organic photovoltaic devices (OPVs) [2], organic field effect transistors (OFETs) [3], organic thin film transistors (OTFTs) [4], and organic light emitting diodes (OLEDs)[5] due to their tunable optical, electrochemical and morphological characteristics. In such devices, optoelectronic properties can be explored through the deposition of semiconducting materials in between of two electrodes.

The most important component is the conjugated backbone in the polymer which can be regulated by physical properties such as π conjugation length, monomer alteration, inter/intramolecular interactions and energy levels [6,7]. One of the most capable methods of lowering the optical and electrochemical band gap of conjugated polymers through the selection of electron donating (donor) and withdrawing unit (acceptor) in an alternating mode in the polymer chain [8,9]. Commonly used donor moieties are thiophene [10], fluorene [5],

dithieno[3,2-*b*:2,3-*d*]silole [11], carbazole [12], dibenzosilole [8], and cyclopentadithiophene groups, While acceptors moieties are generally 2,1,3-benzothiadiazole, thieno[3,4-*b*]thiophene, dioxypyrrolothiophene and diketopyrrolopyrrole (DPP) [3]. Among the donor units, thiophene containing conjugated polymers are widespread attention as novel systems with an excellent hole transporting ability, strong interchain interactions, good light-harvesting properties, great environmental and thermal stability [14,15]. 2,1,3-benzothiadiazole (BT) is a good chromophore and strong electron accepting moiety due to the two electron withdrawing imine groups (-C=N-) which lowers the band gap. And also BT can be possible to form hydrogen bond with adjacent units because of two N atoms in thiazole ring, which could give boost to major planar backbone [16].

Organic-Inorganic hybrid solar cells is one of the alternative solar cells and have attracted to many researchers by trying with new hole transport donor-acceptor materials. Organic-inorganic hybrid material called as perovskite which is new light absorber which contain great properties for the development of low-cost thin film solar cells [17]. The perovskite material performs high absorption coefficient, suitable direct band gap, small exciton binding energies, high carrier mobilities, long diffusion lengths and superior defect tolerances [18]. Moreover, perovskite/HTM polymers solar cells have been developed to achieve high performance. Cai et al showed the PCE upto 18 % for Carbazole and benzothiadiazole based polymers /perovskite solar cells [19]

The present article deals with the synthesis and characterization of new low band gap orange and yellow emitting conjugated polymers (BTTP and BTPCN). BTTP was consisted of repeating units of unsubstituted thiophene and 2,1,3-benzothiadiazole and BTTP-CN was consisted of repeating units of cyano-vinylene based thiophene 2,1,3-benzothiadiazole. BTTP-CN has cyano-substituted vinylene linkages which act as strong electron accepting nature. Due to this nature, it has been extensively adopted in small conjugated molecules [20]. The CN-group can extremely lower the LUMO level and slightly lower the highest occupied molecular orbital (HOMO) level; this can prove by Li and co-workers [21]. When compared to other electron withdrawing moieties, a CN-group containing polymer for photovoltaic properties has only limited success [22]. Accordingly, more examinations may be needed to better understand the photovoltaic properties of CN-group containing

conjugated polymers. The vinylene linkages in the conjugated polymer backbone can give planarity, flexibility and eliminated the torsional strain between donor and acceptor on the entire conjugated system [23]. Structural characterization was carried out using FT-IR, NMR, UV-Vis and Cyclic Voltammetry. The potency of these new polymers (BTTP and BTTP-CN) as hole transport materials (HTM) has been investigated by fabricating organic/perovskite hybrid solar cells. The photovoltaic performance of these device was observed and compared with reference HTM materials of spiro-OMeTAD.

2. Experimental section

2.1. Reagents and solvents

Thiophene 2-carbaldehyde, Zn powder, TiCl_4 , 5-thiophene acetonitrile, potassium *tert*-butoxide, POCl_3 , 4,5-dimethyl-1,2-phenylenediamine, triethylamine, thionyl chloride, N-bromosuccinimide, benzoyl peroxide, triphenylphosphine, sodium hydride were purchased from Sigma-Aldrich, Bangalore, India. Solvents such as THF, DMF, DCM, ethyl acetate, CCl_4 , and acetonitrile respectively were purchased from Sd-fine chemicals, India. All solvents were dried and distilled before the synthesis as per standard procedures.

2.2. Characterization methods

FT-IR analysis was studied through Thermo Nicolet 330 FT-IR spectrometer with KBr pellets with a midrange of ($500\text{-}4000\text{ cm}^{-1}$). The ^1H and ^{13}C NMR spectra were analyzed by using a Bruker Advanced III 400 MHz spectrometer using tetramethylsilane (TMS) as an internal standard. The UV-visible absorption spectra were analyzed on JASCO-V-670 FT-IR spectrometer. The fluorescence emissions were performed with Perkin-Elmer LS45 fluorescence spectrofluorometer. The lifetime measurements were carried out with Jobin Yvon FLUOROLOG-FL3-111 spectrofluorometer. The thin films are spin coated onto a clean glass substrate using apex spin NXG-P1 instrument. A cyclic voltammogram (CV) was recorded on CH-I 660C instrument. Thermal stability was performed on SDT Q600 V20.9 Build 20 instrument under nitrogen flow rate 100 ml/min. The molecular weights of the intermediate compounds were measured from Perkin-Elmer Clarus 680 GC-MS spectrometer and the polymers molecular weight was observed by gel permeation chromatography using a Waters-RID 2414 instrument.

2.4. Photovoltaic device fabrication:

FTO coated glass substrates were etched with Zn powder and acid solution at the concentration of 37% HCl and then cleaned the substrate using detergent and ethanol by sonication. The substrate was then dried by flow gas and exposing to ultraviolet ozone plasma for 15 min. A precursor solution was prepared by mixing 0.6 mL of titanium isopropoxide (TTIP), 0.4 mL of acetyl acetone in 7 mL of isopropanol. 20 μ L of a precursor solution of TiO₂ layer was spin coated at 2800 rpm, and dried it on hot plate at 125°C for 5 min. The mesoporous TiO₂ layer was prepared by diluting the NR30-D paste from Dyesol with ethanol (1:8 mass ratio). 20 μ L of mesoporous TiO₂ was spin coated at 2000 rpm, and dried it again at 125°C for 5 min after that annealed at 540°C for 60 min. The mix solution of perovskite was prepared at a ratio of 1:1 by mole of PbI₂ and CH₃NH₃I in 71 μ L DMSO and 521 μ L DMF as solvent. The perovskite layer was spin coated at 4000 rpm¹ and dried again at 100°C for 15 min. A hole transport material were deposited on perovskite layer by spin coating at 3000 rpm. Finally, the devices were transferred to a thermal–evaporator pump where a thin gold (100 nm) was deposited. The active area of these devices is 18.04 mm².

2.4. Synthetic procedure

2.4.1. Preparation of (E)-1,2bis (5-formyl-2-thienyl)ethylene (Donor-1)

Donor-1 was synthesized and purified according to our published procedures [24]. Firstly the compound 2 was prepared from 2-formyl thiophene (1) using TiCl₄ and Zinc powder under nitrogen atmosphere. Then, compound 2 was formylated using DMF and POCl₃ and refluxed for 15 hr. After the product extracted with dichloromethane anResulting brown colour powder was obtained. Yield: 56.25%, mp: 196-198 °C. FT-IR: (KBr, ν /cm⁻¹): 1647.25 (-C=O), 1454.4 (C-C stretch in aromatic), 958.65 (trans-vinylene). ¹H NMR (CDCl₃, 400 MHz, δ /ppm): 7.20 (d, 2 H, thiophene H), 7.62 (d, 2 H, thiophene H), 7.16 (s, 2 H, vinylene H), 9.80 (s, 2 H, -CHO). ¹³C NMR (CDCl₃, 400 MHz, δ /ppm): 182.62 (-CHO), 150.26, 137.0, 128.28, 142.80 (thiophene C), 124.01 (-CH=CH-). GC-MS calculated for C₁₂H₈O₂S₂ (m/z) = 248, found, 248.80.

2.4.1. Preparation of 2,3-di-thiophen-2-yl-acrylonitrile (4)

Potassium *tert*-butoxide (6 g, 53.49 mmol) was added to a stirred solution of 5-thiophene acetonitrile (3) (5.49 g, 44.58 mmol) which dissolved in ethanol. To this Thiophene 2-carbaldehyde (1) (5 g, 44.58 mmol) was added dropwise and stirred at room temperature for 2 h. The formed yellow color precipitate was filtered and dried. Yield: 8 g, 83.3%. Mp: 110

°C. FT-IR (KBr, v/cm^{-1}): 2208.5 (-CN- stretch), 3080.3 (aromatic C-H stretch), 3097.6 (=C-H stretch). ^1H NMR (400 MHz, CDCl_3 , δ ppm): 7.61 (d, 1H), 7.53 (d, 1H), 7.49 (s, 1H, cyano-vinylene H), 7.34 (d, 1H), 7.29 (d, 1H), 7.14 (t, 1H), 7.06 (t, 1H). ^{13}C NMR (100 MHz, CDCl_3 , δ ppm): 138.7, 137.5, 132.1, 132.0, 129.9, 128.2, 127.9, 126.9 (8C, thiophene C) 125.9 (1C, vinylene C), 116.9 (1C, -CN), 103.1 (1C, vinylene C). GC-MS calculated for $\text{C}_{11}\text{H}_7\text{NS}_2$ (m/z) = 217, found, 217.31.

2.4.2. Preparation of 2,3-bis-(5-formyl-thiophene-2-yl)-acrylonitrile (Donor-2)

The POCl_3 (19.3 ml, 207 mmol) was dropped to DMF (276.1 mmol) at 0 °C over a period of 30 min. Then compound 4 (5 g, 23 mmol) was dissolved in 150 ml of dichloroethane which was added to above-stirred solution and refluxed for 15 h. After completion of the reaction, the crude reaction mixture was quenched with 250 mL water and neutralized to pH 7 by the addition of Na_2CO_3 solution and extracted with dichloromethane. Then dichloromethane layer was dried over NaSO_4 . After solvent evaporation, the crude product was washed twice with diethyl ether. The resulting brown solid was obtained. Yield: 2 g, 31.8%. Mp: 170 °C. ^1H NMR (400 MHz, $\text{DMSO}-d_6$, δ ppm): 9.98 (s, 1H, -CHO), 9.89 (s, 1H, -CHO), 8.34 (s, 1H, cyano-vinylene H), 8.01 (d, 1H), 7.82 (d, 1H), 7.54 (d, 1H), 7.28 (d, 1H). ^{13}C NMR (100 MHz, $\text{DMSO}-d_6$, δ ppm): 184.7, 184.1 (2C, -CHO), 146.7, 142.4, 138.6, 137.1, 136.7, 136.4, 133.6, 128.4 (8C, thiophene C), 126.9 (1C, vinylene C), 116.4 (1C, -CN), 99.9 (1C, vinylene C). HRMS calculated for $\text{C}_{13}\text{H}_7\text{NO}_2\text{S}_2$ (m/z) = 273 found, 272.9920.

2.4.3. Preparation of 5,6-Dimethyl-[2,1,3] benzothiadiazole (6)

4,5-dimethyl-1,2-phenylenediamine (5) (5 g, 36.71 mmol) and triethylamine (18.57 g, 183.55) were dissolved in CH_2Cl_2 (150 mL) and cooled to 0 °C. Thionyl chloride (8.73 g, 73.42 mmol) was slowly dropped to the stirred solution and refluxed for 6 h. After completion of the reaction, the crude mixture was diluted with 300 mL water and extracted with dichloromethane. The organic phase dried over anhydrous Na_2SO_4 . The crude product was purified by using column chromatography on silica gel (1:9 ethyl acetate/hexane as mobile phase). The compound 6 was observed as colorless solid. Yield: 4 g, 66.44%. Mp: 72 °C. ^1H NMR (400 MHz, CDCl_3 , δ ppm): 7.71 (s, 2H, benothiadiazole H), 2.42 (s, 6H, $-\text{CH}_3$). ^{13}C NMR (100 MHz, CDCl_3 , δ ppm): 154.27, 140.53, 119.77 (6C, benothiadiazole C), 20.79 (2C, $-\text{CH}_3$). GC-MS calculated for $\text{C}_8\text{H}_8\text{N}_2\text{S}$ (m/z) = 164, found, 164.80.

2.4.4. Preparation of 5,6-bis(bromomethyl)[2,1,3] benzothiadiazole (7)

Compound 6 (4 g, 24.35 mmol), N-bromosuccinimide (NBS) (8.66 g, 48.71 mmol), and benzoyl peroxide (0.23 g, 0.97 mmol) were dissolved in CCl₄ (100 mL) and refluxed for 6 h. The reaction mixture was cooled and succinimide salt was removed by filtration and the filtrate was evaporated. The compound 7 was observed in the brown color solid. Yield: 6.5 g, 83.4%. Mp: 80 °C. ¹H NMR (400 MHz, CDCl₃, δppm): 8.06 (s, 2H, benothiadiazole H), 4.84 (s, 4H, -CH₂-). ¹³C NMR (100 MHz, CDCl₃, δppm): 154.52, 138.24, 123.55 (6C, benothiadiazole C), 30.08 (2C, -CH₂-). GC-MS calculated for C₈H₆Br₂N₂S (m/z) = 319, found, 319.86.

2.4.5. Preparation of 5,6-bis(triphenylphosphonium di bromomethyl)[2,1,3] benzothiadiazole (Acceptor-1)

Compound 7 (2 g, 6.25 mmol), and triphenylphosphine (3.44 g, 13.13 mmol) were dissolved in 1:9 ratio of CH₃CN (100 mL) and CH₂Cl₂ (10 mL). The resulting suspension was stirred at room temperature for overnight. The formation of a colorless precipitate was filtered and washed twice with diethyl ether. Yield: 4.24, 80%. FT-IR (KBr, v/cm⁻¹): 3053.3 (aromatic C-H stretch), 1739.7 (C=C bending), 1435.0 (aromatic C-C stretch), 1585.4 (C=N stretch), 742.59 (C-P), 686.6 (C-Br). ¹H NMR (400 MHz, DMSO-d₆, δppm): 7.94-7.57 (m, 32H, phenyl ¹H), 4.75 (s, 4H, -CH₂-). ¹³C NMR (100 MHz, DMSO-d₆, δppm): 152.64, 135.39, 134.07, 133.97, 130.32, 130.20, 129.36, 125.1, 117.53, 116.6 (aromatic C), 30.6 (2C, -CH₂-). HRMS calculated for C₄₄H₃₆Br₂N₂P₂S (m/z) = 844 found, 844.0438.

2.4.6. General procedure for the synthesis of polymers

Acceptor-1 (2.1 g, 2.48 mmol) was dissolved in 100 mL of anhydrous THF. To this 60% sodium hydride (3.96 g, 99.22 mmol) was added as portion wise, and the color of reaction mixture was changed from colorless to a purple color. After donor-1 or 2 (1.23 g, 4.96 mmol) was added portion wise to the reaction mixture and reflux for overnight. The reaction mixture was cooled to room temperature, diluted with ice cold water and extracted with ethyl acetate. After solvent evaporation, the crude product was recrystallized from isopropanol.

BTTP: Red color solid, FT-IR (KBr, v/cm⁻¹): 3012 (aromatic C-H stretch), 1656 (-C=C- stretch in conjugation), 1531 (aromatic C=C stretch), 931 (*trans*-vinylene) ¹H NMR (400

MHz, DMSO- d_6 , δ ppm): 7.65-7.59 (br, thiophene H), 7.59-7.57 (br, benzothiadiazole H), 7.57-7.50 (br, vinylene H).

BTTP-CN: Brown colour solid, FT-IR (KBr, ν/cm^{-1}): 3018 (aromatic C-H stretch), 2210 (-CN group), 1739 (C=C-CN stretch), 1587 (aromatic C=C stretch). ^1H NMR (400 MHz, DMSO- d_6 , δ ppm): 7.64-7.59 (br, thiophene H), 7.59-7.57 (br, benzothiadiazole H), 7.57-7.51 (br, vinylene H).

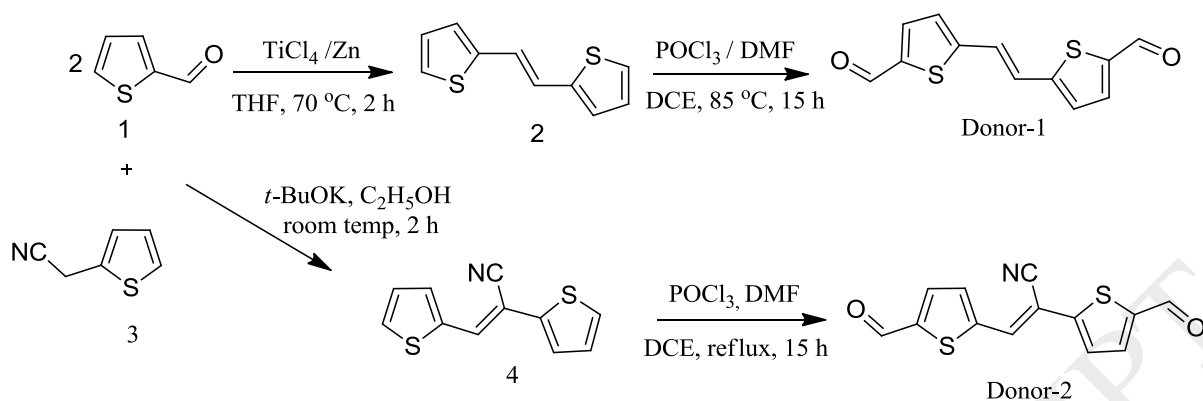
3. Results and Discussion

3.1. Synthesis and characterization of monomers and polymers

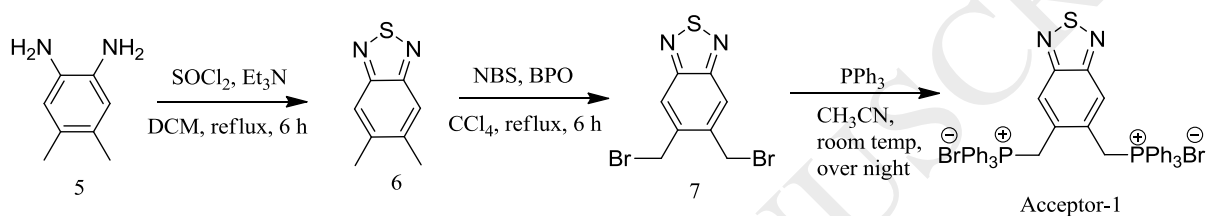
The general synthetic strategy for the establishing monomers and two polymers are outlined in the **scheme. 1**. The structures of both monomers and target polymers were confirmed by FT-IR and ^1H NMR spectroscopic techniques. Firstly, the thiophene donor type of intermediate (2) was synthesized from commercially available 2-thiophene carboxaldehyde (1) using Zn powder, TiCl_4 via McMurry coupling reaction as follows to that reported literature [24]. Newly formed vinyl linkage signal appeared at 7.0 ppm ($J=14$) in ^1H NMR which indicates the intermediate (2) was in *trans*-configuration. The cyano containing intermediate (4) was synthesized from compound (1) and 2-thiopheneacetonitrile (3) using *t*-BuOK as a base. Resulting cyano-vinylene bond was confirmed by appearing the sharp absorption band at 2208.5 in FT-IR. The Donors and acceptor were synthesized from intermediates (2 & 4) by well-known Vilsmeier-Haack reaction. Both monomers contain aldehyde functional groups were observed at 1647.20, 1645.28 cm^{-1} in FT-IR, aldehyde protons, and carbon signals appeared at 9.80, 9.89, 9.98 and 182, 184.1, 184.7 ppm in ^1H and C^{13} NMR spectrum. These values were confirmed for the formation of formyl thiophene group (Donor-1 and 2).

Secondly, in the part of acceptor side, Dimethyl benzothiadiazole (6) was synthesized from reported literature [25]. Bromomethyl 2,1,3-Benzothiadiazole was firstly synthesized using *N*-bromosuccinimide (NBS) reagent and benzoyl peroxide as an initiator. This was confirmed by appearance of $-\text{CH}_2\text{-Br}$ signal at 4.84 ppm in ^1H NMR, and then directly converted to monomer (M_3) by treatment with triphenylphosphine. The structure of M_3 was confirmed by appearing the sharp absorption bands at 742.59 (C-P stretching), 686.66 (C-Br stretching) in FT-IR and 7.94-7.57 ppm (32 phenyl hydrogens of phosphonium salt) in ^1H NMR spectra.

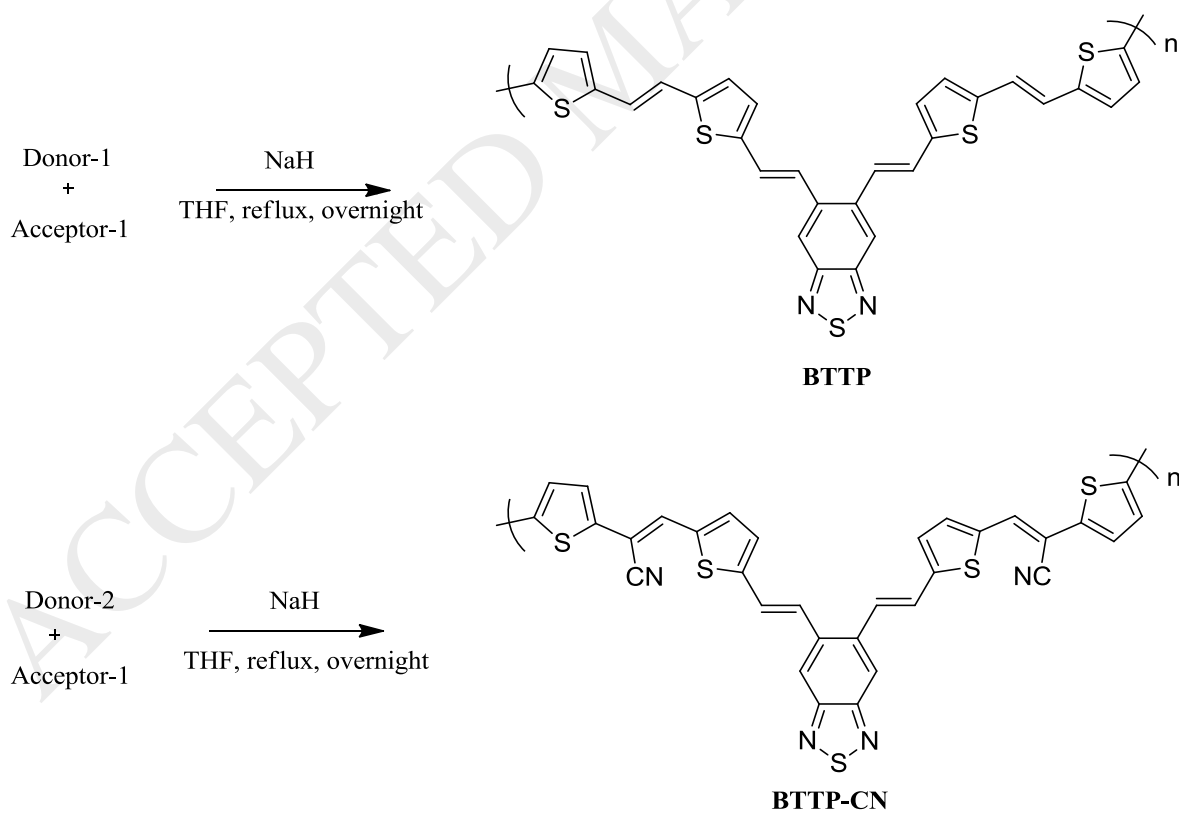
Synthesis of donor moieties:



Synthesis of acceptor moiety:



Synthesis of polymers:



Scheme 1: Synthetic reaction of donors, acceptors and polymers

3.2. Structural Characterization of the polymers (BTTP and BTTP-CN)

The synthetic procedures of both polymers (BTTP, BTTP-CN) are sketched in Scheme 1. Both polymers were synthesized from the thiophene dicarbonyl monomers (Donor-1 & 2) and benzothiadiazole phosphonium salt monomer (Acceptor) in dry THF solvent using popular Wittig condensation reaction followed by Sodium hydride as a base for deprotonation of phosphonium salt. The structural characteristics of both polymers were verified from FTIR and NMR spectroscopy.

BTTP and BTTP-CN are interesting conjugated conductive polymers containing an electron pair donating nitrogen atoms. The polymers were investigated by FT-IR spectra which are shown in **Fig. 1**. Both polymers (BTTP, BTTP-CN) showed characteristic absorption bands at 3012.8, 3018.6 cm^{-1} which indicated for thiophene C-H stretching, 1656, 1730 cm^{-1} was represented for -C=N- stretching in benzothiadiazole, 1531.4, 1587 cm^{-1} was represented for -C=C- stretching. In BTTP-CN, the medium absorption peak at 2220 cm^{-1} was represented for the -CN group. The absorption at 931, 939 cm^{-1} was denoted that trans-vinylene was predominant among newly formed vinylene double bonds. These values are suggested for the successful reaction of donors with acceptor.

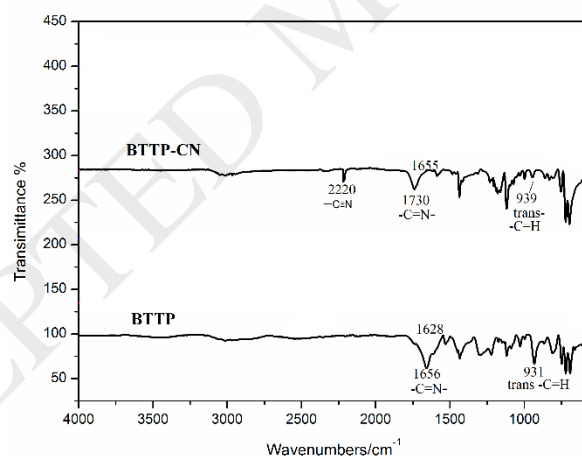


Fig. 1. FT-IR spectra of the polymers

Both ^1H NMR spectra of the polymers are shown in **Fig. 2**. All thiophene protons of both polymers were shown broad peak signal in between of 7.64-7.59 ppm. The benzene protons signal of the benzothiadiazole group was formed at 7.59-7.57 ppm. The broad signal formed at 7.57-7.50 due to vinylene protons. Both polymers were exhibited good solubility in THF, chloroform, and limited solubility in halo substituted benzenes at room temperature. Complete solubility could be achieved by elevated temperatures.

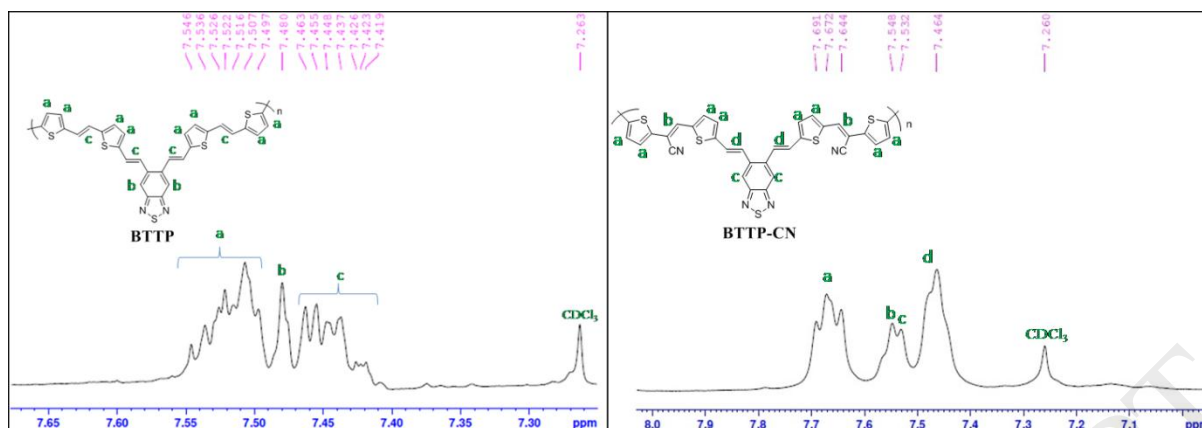


Fig. 2. ^1H NMR spectra of both polymers.

The number average (M_n), weight average molecular weight (M_w) and polydispersity index (PDI) were measured by gel permeation chromatography (GPC) against polystyrene standards using THF as eluent. BTTP has received higher molecular weight (M_n) as 20553 Da with PDI of 1.41 and for BTTP-CN has been found M_n was 9526 Da with PDI of 1.21

3.5. Optical properties

3.5.1. Absorption spectra

The optical related properties of both polymers were explored by UV-vis absorption spectroscopy. The absorption spectra of the both polymers were measured in chloroform solvent (5×10^{-5} M) and thin films which are shown in **Fig. 3** and the values indicated in Table 1. The absorption peaks of both polymers were appeared at short (high energy band) wavelength because of π - π^* transition and long wavelength (low energy band, n - π^*) regions because of internal charge transfer (ICT) [26]. This is the common feature in conjugated polymers due to donor-acceptor orbital hybridization [27]. In solution, BTTP polymer was shown absorption peak at 266 nm and BTTP-CN polymer shown absorption at 317 nm which due to the π - π^* transition band. BTTP showed broad absorption peak in the range of 320-550 nm with 403 nm of absorption maxima and BTTP-CN showed absorption peak at 397 nm related to n - π^* transition. Based upon these results unsubstituted vinylene link polymer (BTTP) was shown 10 nm of bathochromic shift than cyano substituted vinylene polymer (BTTP-CN). In thin films, both copolymers were displayed similar broadening of absorption peaks and maxima. BTTP and BTTP-CN exhibited a bathochromic shift in thin film absorption onset (560 nm and 580 nm). It could be due to solid state effect and aggregation π -

π stacking occurred between polymer chains [28]. The band edge of the polymer (BTTP) thin film was observed at 560 nm and the corresponding optical band gap was 2.2 eV. But, in the case of cyano substituent polymer possess the band edge was 580 nm and the corresponding optical band gap was 2.13 eV. Lesser band gap in the solid state of the polymer enhance intramolecular charge transfer between thiophene donor and thiazole acceptors.

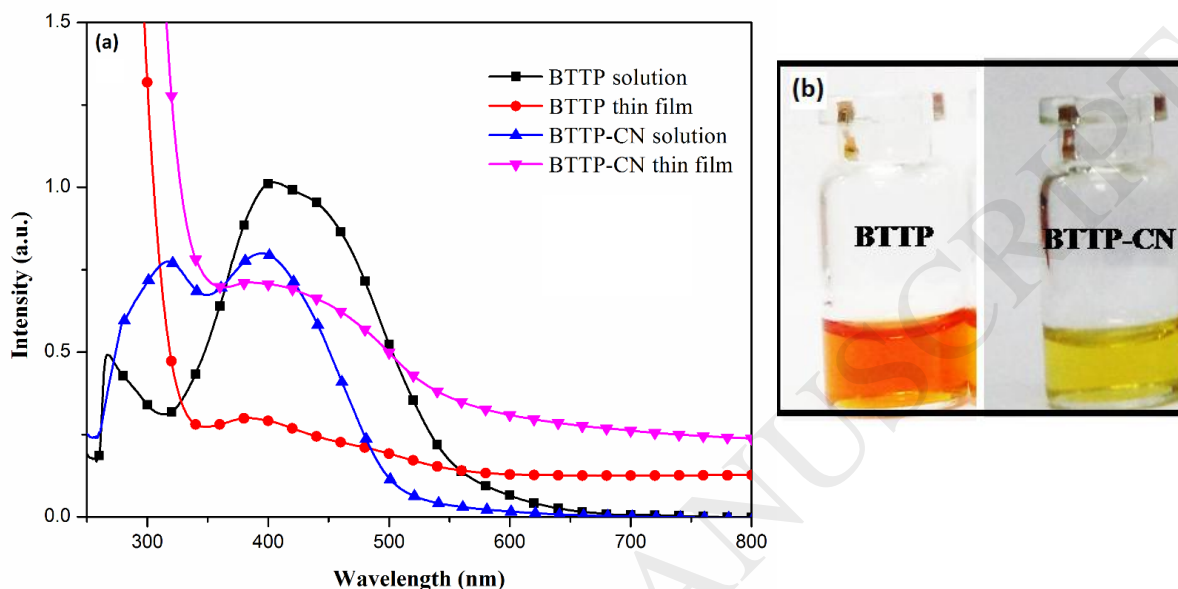


Fig. 3 (a) Absorption spectra of the polymers in CHCl_3 and thin film state (b) Visual change photos of both polymers under daylight

Figure 4 shows diffuse reflectance (DR) spectra of powdery polymers of BTTP and BTTP-CN. Broader DR spectra was able to observe for both polymers (BTTP and BTTP-CN) and observed in the range of 350-500 nm. The absorption band of the BTTP and BTTP-CN were 396 and 392 nm which seems to be shifted to longer wavelengths compared to solution state of the polymers. These polymers were exhibited the peaks at different position from those observed with the solution and thin film state which suggest a strong intermolecular electronic interaction between donor and acceptor moieties.

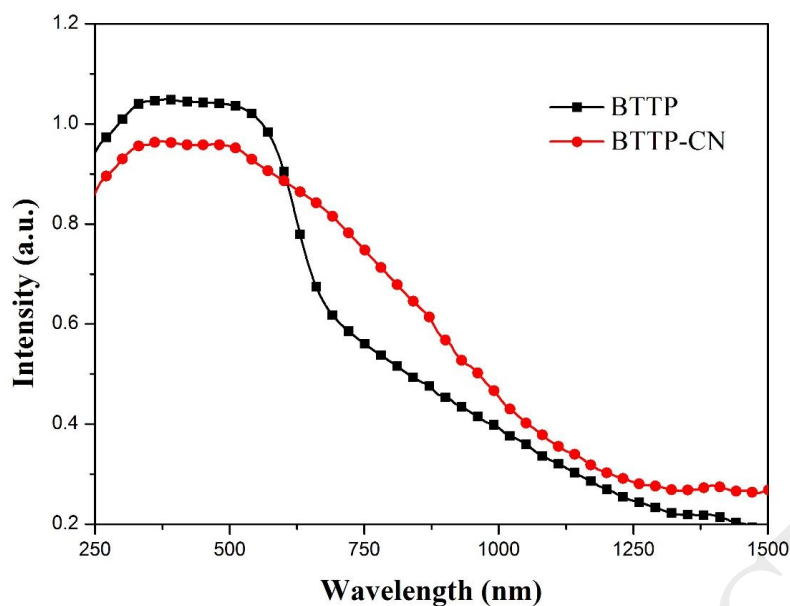


Fig. 4. Diffuse reflectance (DR) spectra of the polymers

3.5.2. Fluorescence spectra

Fig. 5 depicts the fluorescent emission spectra of both polymers in chloroform and spin coated films. In a solution state, the polymer without cyano group (BTTP) showed strong orange fluorescent colour with emission maxima at 585 nm and with cyano polymer (BTTP-CN) exhibited yellowish fluorescent colour with emission maxima at 520 nm. The emission spectra of the polymers in film state is much broadened than the emission from thin films. The excitation spectrum of the both polymers for the emission wavelength gives the information about π - π^* transitions results in more intense fluorescence emission. The emission maximum of the polymers is bluishifted compared to solid state of the polymer which was noticed at 580 nm and 650 nm for BTTP-CN and BTTP polymers. Fluorescence emission of cyano substituent polymer is strongly blue shifted than polymer without cyano. This may be caused by the strong intramolecular charge transfer (ICT) between thiophene and benzthiadiazole group. ICT is much stronger in cyano containing polymers because of dicyanovinyl group is much stronger electron acceptor. [29]

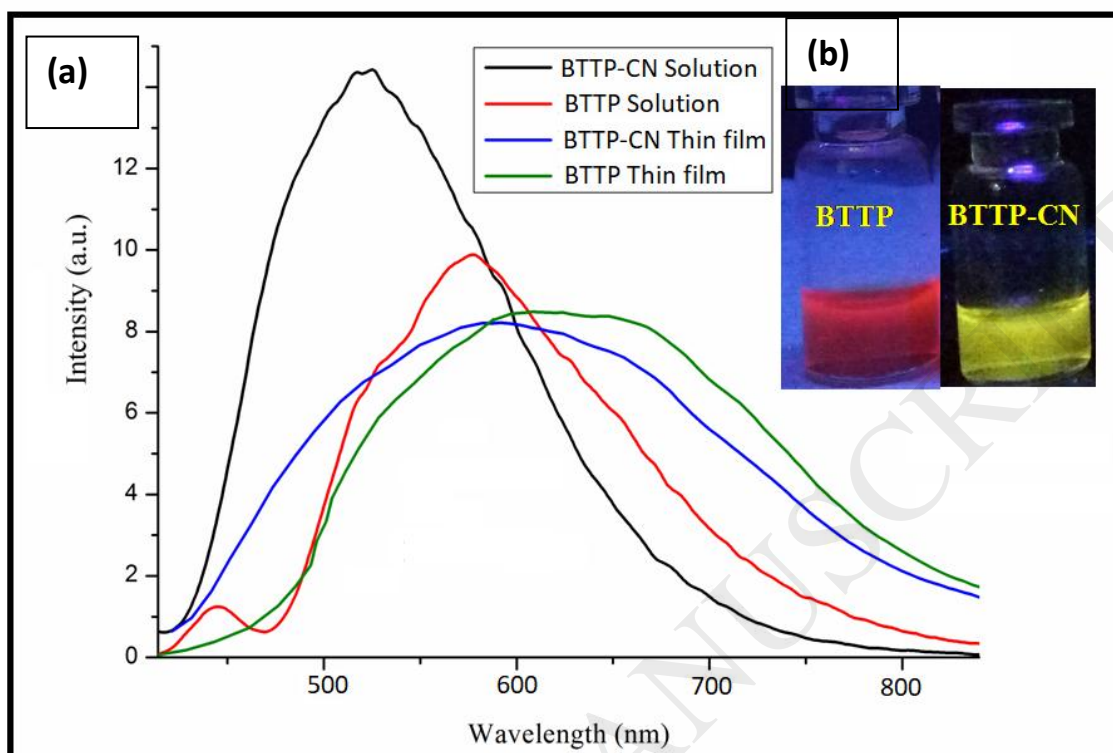


Fig. 5 (a) Fluorescence spectra of the polymers in CHCl_3 and thin film state (b) Visual change photos of both polymers under UV light

The wave length gap between the absorption maxima and fluorescence maxima is called the Stokes shift. The luminescence property is depending upon the Stokes shift value. The decreased luminescence of polymers is due to lower stokes shift, because of self-absorbing the emitted light. The Stokes shift was determined according to the given formula.

$$\Delta\lambda_{\text{Stokes}} = \lambda_{\text{max. emission}} - \lambda_{\text{max. absorption}} \quad (1)$$

Stokes shift of BTTP and BTTP-CN was calculated as 182 nm and 123 nm. Both polymers were exhibited higher Stokes shift values than previously published thiophene-thiazole based oligomers [25]. The large Stokes shift is in favor of practical applications since it can decrease self-quenching and increase the luminescence [30]. From the optical properties of both polymers, it is noticeable that the interaction between donor and acceptor backbone greatly depends on several aspects such as attachment of donor-acceptor, their strength, steric hindrance and planarity of the polymer backbone.

Table. 1 Comparative spectral analysis of both polymers (BTTP and BTTP-CN).

| Measurement | Properties | BTTP | BTTP-CN |
|-------------------------------|------------------------|-----------------------|-----------------------|
| Absorption spectra | Absorption maxima (nm) | 266 ,403 | 317,397 |
| | UV-Onset absorption | 560 | 580 |
| | Optical Band gap (eV) | 2.2 | 2.13 |
| Fluorescence Spectra | Emission maxima (nm) | 585 | 520 |
| | Stokes Shift (nm) | 182 | 123 |
| Electrochemical (CV) | E_{onset}^{ox} (V) | 1.00 | 0.85 |
| | E_{onset}^{red} (V) | -0.90 | -0.75 |
| | HOMO (eV) | -5.40 | -5.25 |
| | LUMO (eV) | -3.50 | -3.65 |
| | E_g^{Ec} (eV) | 1.90 | 1.60 |
| Fluorescence Life time | Analysis | Bi-exponential | Bi-exponential |
| | Lifetime (ns) | $\tau_1 = 1.05$ | $\tau_1 = 0.72$ |
| | | $\tau_2 = 2.18$ | $\tau_2 = 3.06$ |
| | | $\tau_3 = \text{Nil}$ | $\tau_3 = \text{Nil}$ |
| | Amplitude | $A_1 = 49.87$ | $A_1 = 67.60$ |
| $A_2 = 50.13$ | | $A_2 = 32.40$ | |
| χ^2 | 1.26 | 1.67 | |

3.5.3. Fluorescence lifetime measurement

Fluorescence lifetime was evaluated to find the time of the present polymer spends time in the excited state before coming to the ground state. **Fig. 6** shows typical fluorescence lifetime (decay time) spectra of the polymers BTTP and BTTP-CN with the emission wavelengths of 585 and 520 nm. Both polymers of nanosecond time profiles were calculated by utilizing a time-correlated single photon counting method [31]. Exploration of the polymers decay curves confirmed that it could be fitted completely with that two exponential decay function of the form (2) and tri-exponential decay function of the form (3).

$$F(t) = A_1 e^{\frac{-t}{\tau_1}} + A_2 e^{\frac{-t}{\tau_2}} \quad (2)$$

$$F(t) = A_1 e^{\frac{-t}{\tau_1}} + A_2 e^{\frac{-t}{\tau_2}} + A_3 e^{\frac{-t}{\tau_3}} \quad (3)$$

Where ‘A’ is the amplitude of fluorescence intensity at time zero and ‘ τ ’ is fluorescence lifetime. Bi-exponential curves was calculated from the parameters for BTTP and BTTP-CN which are displayed in **Table 1**. The assertive first lifetime (τ_1) of BTTP is 1.05 ns and a second lifetime $\tau_2 = 2.18$ ns have the lowest χ^2 fit (1.26). The reduced first lifetime (τ_2) for BTTP-CN is 0.72 ns and a second lifetime $\tau_2 = 3.06$ ns have the 1.67 χ^2 fit.

The nature of the fit was determined by the examination of the residuals, and the value of the lower χ^2 ratio [31].

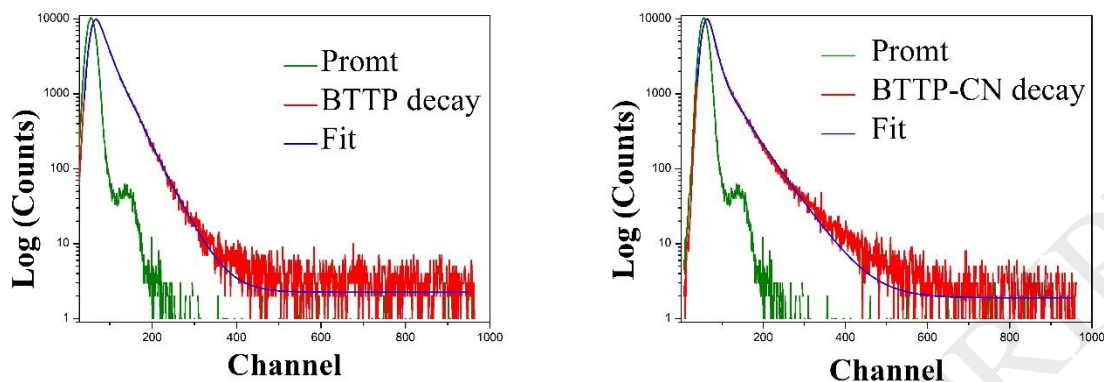


Fig. 6. Fluorescence Lifetime spectrum of the polymers BTTP and BTTP-CN

3.6. Electrochemical measurements

The electrochemical properties of both copolymers were investigated by cyclic voltammetry. By utilizing this technique HOMO and LUMO energy levels of polymers can be determined. These energy levels are necessary for calculating the electrochemical band gap of the polymers. The cyclic voltammetry studies were carried out in a 0.1 mol/L tetrabutylammonium hexafluorophosphate (Bu_4NPF_6) solution in CH_3CN at ambient temperature using 50 mV/s scan rate under room temperature. An ITO plate used as a working electrode. It is coated with the polymer thin film by drop casting method. The Bu_4NPF_6 used as a supporting electrolyte, Ag/AgCl as a reference electrode and platinum wire used as a counter electrode. The HOMO, LUMO and electrochemical band gap (E_g^{ec}) value of both polymers were estimated using the reported empirical equation [32].

$$E_{\text{HOMO}} = -(E_{\text{ox}} + 4.4) \quad (4.1)$$

$$E_{\text{LUMO}} = -(E_{\text{red}} + 4.4) \quad (4.2)$$

$$E_g = E_{\text{HOMO}} - E_{\text{LUMO}}. \quad (4.3)$$

Fig. 7 shows the cyclic voltammograms of BTTP and BTTP-CN polymers. Clearly, both polymers have positive (oxidation) and negative (reduction) peaks which indicate the great combination of donor and acceptor units in the system. While introducing the electron-withdrawing elements such as cyano group at vinyl position of electron accepting block can

tune the HOMO and LUMO energy levels of the polymers resulted lower band gap. The onset oxidation (E_{ox}) and reduction (E_{red}) potentials of BTTP were 1.0 and -0.9 V respectively. The HOMO and LUMO energy levels were -5.40 and -3.50 eV respectively and electrochemical energy band gap was 1.9 eV. The onset oxidation (E_{ox}) and reduction (E_{red}) potentials of BTTP-CN were 0.85 V and -0.75 V respectively. The HOMO and LUMO energy levels of BTTP-CN were -5.25 and -3.65 eV with electrochemical energy band gap was 1.6 eV. The cyano substituted polymer (BTTP-CN) showed significantly reduced LUMO energy level compared with polymer (BTTP). The HOMO energy levels of the new polymers were mainly related to the donor moiety but could also be affected by acceptor moiety. BTTP-CN displayed slightly increased HOMO energy levels compared with BTTP polymer. Because of lower electrochemical band gap, these polymers could be employed in solar cell applications.

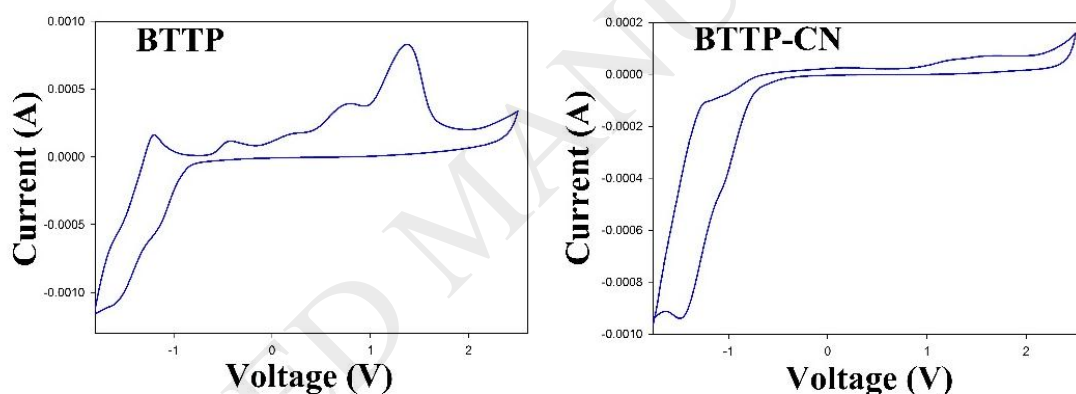


Fig. 7. Cyclic voltammograms of the polymers (BTTP and BTTP-CN) sample thin films on ITO glass in 0.1 M Bu_4NPF_6 of CH_3CN solution with a scan rate of 50 mV/s.

3.7. Thermal analysis

Thermogravimetric analysis (TGA) is important and useful dynamic way to distinguish the degradation nature of the polymers. Thermal stability or degradation for the conjugated polymers is essential characterization for their potential applications. The thermal stability of both polymers is displayed in **Fig. 8**. Two stages of thermal decomposition were exhibited by both polymers. For BTTP, the first thermal decomposition temperature with 10% weight loss at 220 °C. The second stage of thermal decomposition began at 325 °C and

continued up to 800 °C with 75% weight loss. For BTTP-CN, the first thermal decomposition temperature with 10% weight loss at 254 °C. The second stage of thermal decomposition began at 325 °C and continued up to 800 °C with 90% weight loss. Among these two polymers, BTTP-CN has high thermal stability due to a cyano group, because the strong electron withdrawing nature of cyano group can increase the stabilization of the frontier molecular orbitals for semiconducting polymeric materials. Furthermore, it extended a strong intermolecular interaction [33, 34]. Definitely, the thermal stability of both polymers is capable for their applications in optoelectronic devices.

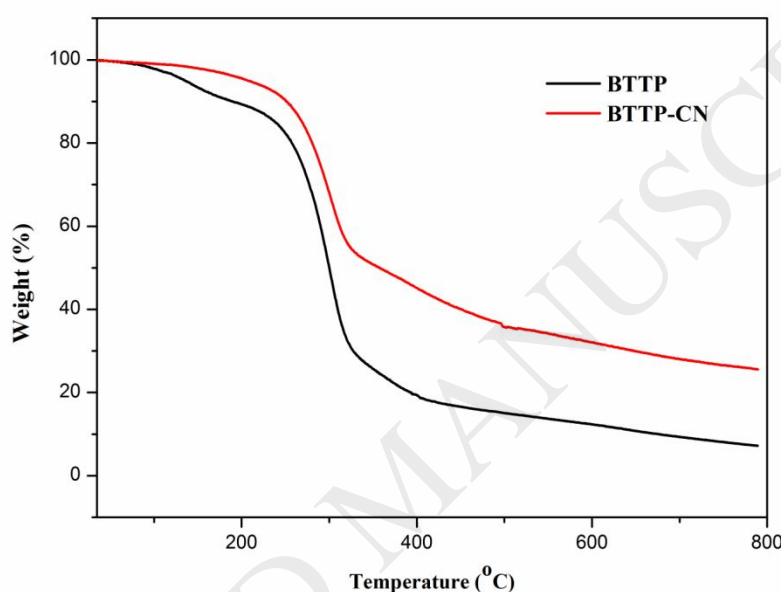


Fig. 8. TGA curve of BTTP and BTTP-CN at a heating rate of 10 °C min⁻¹ under nitrogen.

3.9. Photovoltaic properties

We have also investigated the potentiality of these thiophene and benzothiadiazole based conjugated polymers (BTTP and BTTP-CN) as hole transporting materials (HTM) in hybrid perovskite solar cells (PSC). The general device structure is given in **Fig. 9** (left). The PSC is composed of an FTO/glass substrate covered successively by a thin compact *c*-TiO₂ (50 nm thickness) and then a mesoporous *mp*-TiO₂ layers (200 nm thickness). The solution containing CH₃NH₃I + PbI₂ is then spin coated on the glass/*c*-TiO₂/*mp*-TiO₂ film, followed by a thermal annealing to form the perovskite absorbing layer (400 nm thickness). Finally, hole transport layer is spin coated (200 nm thickness) and a thin layer of Au was deposited by thermal evaporation to serve as cathode. The energy level alignment of different device components used in our study is displayed in **Fig. 9** (right). The Spiro-OMeTAD (2,2',7,7'-

Tetrakis-(N,N-di-4-methoxyphenylamino)-9,9'-spirobifluorene) without additive is used as control material and its HOMO/LUMO characteristics are taken from our previous reported results [35].

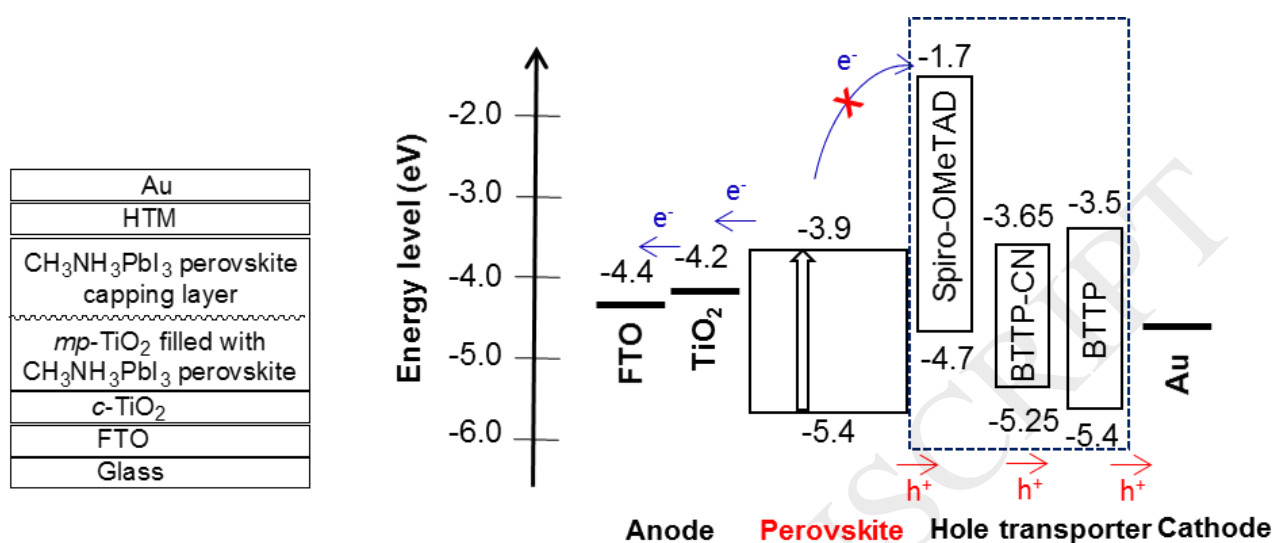


Fig. 9. General solar cell device structure (left) and energy level alignment of different device components (right).

As shown in **Fig. 9**, the HOMO levels of **BTTP** and **BTTP-CN** are a little bit higher than that of the CH₃NH₃PbI₃ perovskite material, suggesting that hole charge are able to be transferred from perovskite to the two polymers at their interfaces. In other hand, their LUMO energy levels are located higher than that of perovskite, suggesting that **BTTP** and **BTTP-CN** could have electron-blocking property. But reasonably, HOMO energy differences is not so big and we cannot exclude a non-negligible recombination state at HTM/perovskite.

The perovskite-based solar cells were elaborated using **BTTP**, **BTTP-CN**, and **Spiro-OMeTAD** as hole-transporting materials. It is well known that pristine organic semiconducting materials have low conductivity and hole mobility, leading to poor perovskite solar cell performance. The most popular HTM dopants are bis(trifluoromethane)sulfoimide (LiTFSI) and tert-butylpyridine (tBP). The latter increases the mobility of the charge carriers [36] and the former increases the carrier density [37]. However, both contribute also largely to the degradation of the stability of perovskite material [38,39]. For this reason, developing HTM working without any additive is a promising approach to enhance the long-term stability of the PSC device.

The J-V curves of the best devices are shown in **Fig. 10** and the photovoltaic outputs are tabulated in the **Table 2**. The control device using doped Spiro-OMeTAD HTM gave a photocurrent density (J_{sc}) of 21.93 mA.cm⁻², fill factor (FF) of 0.62 and an open circuit voltage (V_{oc}) of 0.92 V, corresponding to the power conversion efficiency (PCE) of 12.53 %. The device using pristine Spiro-OMeTAD without any additive gave poorer photovoltaic performance (7.55 %), mostly due to lower photocurrent. This demonstrates the effects of additive in increasing the performance of PSC as reported in our previous work [40]. Herein the photovoltaic performance of Spiro-OMeTAD based device validated our device elaboration procedure.

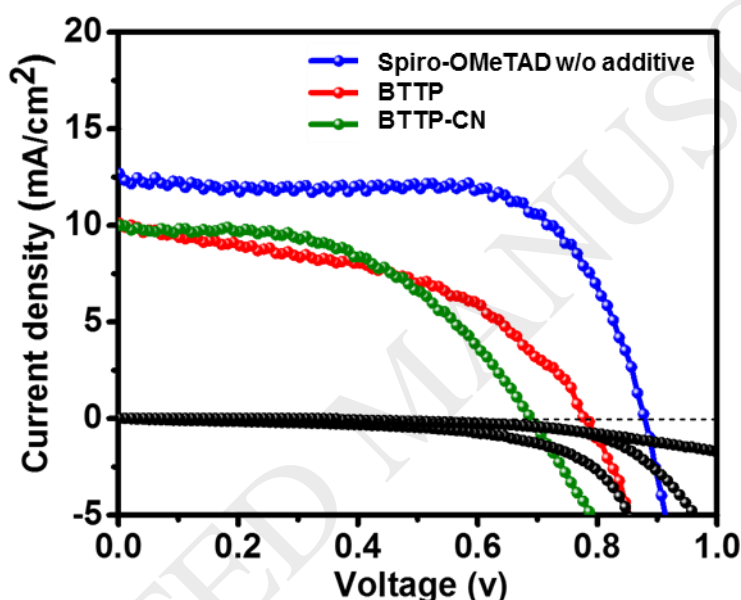


Fig. 10. J-V curves of the devices based on FTO/bl-TiO₂/m-TiO₂/MAPbI₃/HTM/Au device structure under illumination and in the dark: BTTP (red) and BTTP-CN (blue).

Table 2. Photovoltaic parameters derived from J-V measurements

| Devices | J_{sc} (mA/cm ²) | V_{oc} (V) | FF | PCE (%) |
|---------------------------|-----------------------------------|-----------------|-------|------------|
| Spiro-MeOTAD | 21.93 | 0.920 | 0.620 | 12.53 |
| Spiro-MeOTAD w/o additive | 12.69 | 0.880 | 0.676 | 7.55 |
| BTTP in Chloroform | 10.11 | 0.780 | 0.482 | 3.80 |

| | | | | |
|-----------------------|-------|-------|-------|------|
| BTTP-CN in Chloroform | 10.01 | 0.690 | 0.503 | 3.48 |
|-----------------------|-------|-------|-------|------|

The **BTTP** based device delivered a J_{sc} of $10.11 \text{ mA}\cdot\text{cm}^{-2}$, a V_{oc} of 0.78 V , and an FF of 0.48 , corresponding to a PCE of 3.80% . **BTTP-CN** exhibited a J_{sc} of 10.01 , a V_{oc} of 0.69 V and an FF of 0.50 leading to a PCE of 3.5% . Despite a better FF compared to that of **BTTP**, **BTTP-CN** photovoltaic performance is poorer than that of **BTTP** due to lower J_{sc} and V_{oc} . Although more effort should be made to understand the role of thiophene and benzothiadiazole based conjugated polymers **BTTP** and **BTTP-CN** HTM layer in the PSC photovoltaic performance, we thus attributed this difference in photovoltaic performance to both low charge carrier mobility of pristine **BTTP** and **BTTP-CN** and certainly a non-negligible recombination ratio at HTM/perovskite interface which causes directly the low photocurrents observed. Moreover, chloroform used as the most efficient HTM solvent is not the most adequate for high efficient PSC elaboration. However, these preliminary results show the potentiality of solution processable **BTTP** and **BTTP-CN** as HTM for hybrid photovoltaics.

4. Conclusion

In summary, thiophene and benzothiadiazole based conjugated polymers (**BTTP**, **BTTP-CN**) with and without cyano group has been synthesized with several schematic steps. The Donors, acceptors and Polymers were characterized using FTIR, NMR, Mass and GPC technique. These polymers are soluble in common organic solvents such as THF and CHCl_3 which allows to use as thin films in the elaboration of electronic devices. **BTTP** has emitted strong orange colour and cyano substituted **BTTP** emitted yellowish colour with maxima of 520 nm . Cyano substituent has placed very important role in the conjugated polymers (**BTTP**) to reduced band gap (1.6 eV), fluorescence life time (0.72 ns), higher thermal stability ($325 \text{ }^\circ\text{C}$), increased HOMO level (-5.25eV), decreased LUMO level (-3.65). Overall, both polymers have numerous potential applications in the field of photovoltaics, OLEDs, and nonlinear optics. Ability of new polymers as hole transporting materials in perovskite solar cells has been analyzed. **BTTP** has shown better photovoltaic performance (PCE: 3.8%) than **BTTP-CN** and this was very less compared to Spiro-OMeTAD based device. In future, these polymers maybe doped with various Lewis acid to increase conductivity and able to improve the photovoltaic performance of perovskite solar cells.

Acknowledgement

This work was financially supported by DST-SERB, New Delhi (Grant no. SB/FT/CS-140/2013). The authors are grateful to DST/VIT-FIST, VIT University for providing instrumental facilities.

References

- [1] D.H. Yun, H.S. Yoo, S.W. Heo, H.J. Song, D.K. Moon, J.W. Woo, Y.S. Park, Synthesis and photovoltaic characterization of D/A structure compound based on N-substituted phenothiazine and benzothiadiazole, *J. Ind. Eng. Chem.* 19 (2013) 421-426.
- [2] S. Goker, G. Hizalan, E. Aktas, S. Kutkan, A. Cirpan, L. Toppare, 2, 1, 3-Benzooxadiazole, thiophene and benzodithiophene based random copolymers for organic photovoltaics: thiophene versus thieno [3, 2-b] thiophene as π -conjugated linkers, *New J. Chem.* 40 (2016) 10455-10464.
- [3] J. Yuan, X. Huang, F. Zhang, J. Lu, Z. Zhai, C. Di, W. Ma, Design of benzodithiophene-diketopyrrolopyrrole based donor-acceptor copolymers for efficient organic field effect transistors and polymer solar cells, *J. Mater. Chem.* 22 (2012) 22734-22742.
- [4] M.C. Hwang, J.W. Jang, T.K. An, C.E. Park, Y.H. Kim, S.K. Kwon, Synthesis and characterization of new thermally stable poly (naphthodithiophene) derivatives and applications for high-performance organic thin film transistors, *Macromolecules.* 45 (2012) 4520-4528.
- [5] H. Shi, J. Yuan, X. Wu, X. Dong, L. Fang, Y. Miao, F. Cheng, H. Shi, J. Yuan, X. Wu, X. Dong, L. Fang, Y. Miao, F. Cheng, Two novel indolo [3, 2-b] carbazole derivatives containing dimesitylboron moieties: synthesis, photoluminescent and electroluminescent properties, *New J. Chem.* 38 (2014) 2368-2378.
- [6] D. Dang, M. Xiao, P. Zhou, J. Shi, Q. Tao, H. Tan, R. Yang, Manipulating backbone structure with various conjugated spacers to enhance photovoltaic performance of D-A-type two-dimensional copolymers, *Org. Electron.* 15 (2014) 2876-2884.
- [7] G. Zuo, Z. Li, M. Zhang, X. Guo, Y. Wu, S. Zhang, Influence of the backbone conformation of conjugated polymers on morphology and photovoltaic properties, *J. Hou, Polym. Chem.* 5 (2014) 1976-1981.
- [8] H.J. Song, J.Y. Lee, E.J. Lee, D.K. Moon, Conjugated polymer consisting of dibenzosilole and quinoxaline as donor materials for organic photovoltaics, *Eur. Polym. J.* 49 (2013) 3261-3270.
- [9] M.L. Keshtov, D.V. Marochkin, V.S. Kochurov, A.R. Khokhlov, E.N. Koukaras, G.D. Sharma, New conjugated alternating benzodithiophene-containing copolymers with different acceptor units: synthesis and photovoltaic application, *J. Mater. Chem. A.* 2 (2014) 155-171.

- [10] B. Zaifoglu, M. Sendur, N.A. Unlu, L. Toppare, High optical transparency in all redox states: Synthesis and characterization of benzimidazole and thieno [3, 2-b] thiophene containing conjugated polymers, *Electrochim. Acta.* 85 (2012) 78-83.
- [11] J.H. Kim, K.H. Kim, J. Shin, T.W. Lee, M.J. Cho, D.H. Choi, Electrical and photoelectrical properties of polymer single nanowire made of diketopyrrolopyrrole-based conjugated copolymer bearing dithieno [3, 2-b: 2', 3'-d] thiophene, *Synth. Met.* 167 (2013) 37-42.
- [12] A. Upadhyay, S. Karpagam, Synthesis and photo physical properties of carbazole based quinoxaline conjugated polymer for fluorescent detection of Ni²⁺, *Dyes. Pigments.* 139 (2017) 50-64.
- [13] T. Ikai, R. Kojima, S. Katori, T. Yamamoto, T. Kuwabara, K. Maeda, S. Kanoh, Thieno [3, 4-b] thiophene–benzo [1, 2-b: 4, 5-b'] dithiophene-based polymers bearing optically pure 2-ethylhexyl pendants: Synthesis and application in polymer solar cells, *Polymer.* 56 (2015) 171-177.
- [14] Y. Zou, A. Najari, P. Berrouard, S. Beaupre, B. Reda Aich, Y. Tao, M. Leclerc, A thieno [3, 4-c] pyrrole-4, 6-dione-based copolymer for efficient solar cells, *J.Am. Chem. Soc.* 132 (2010) 5330-5331.
- [15] L. Huo, J. Hou, S. Zhang, H.Y. Chen, Y. Yang, A Polybenzo [1, 2-b: 4, 5-b'] dithiophene Derivative with Deep HOMO Level and Its Application in High-Performance Polymer Solar Cells, *Angew. Chem. Int. Ed.* 49 (2010) 1500-1503.
- [16] X. Huang, G. Zhang, C. Zhou, S. Liu, J. Zhang, L. Ying, Y. Cao, Tailoring π -conjugated dithienosilole–benzothiadiazole oligomers for organic solar cells, *New J. Chem.* 39 (2015) 3658-3664.
- [17] M.I. Ahmed, A. Habib, S.S. Javaid. Perovskite solar cells: potentials, challenges, and opportunities. *Int J Photo energy* (2015) 2015:592308.
- [18] Z. Liu, Q. Chen, Z. Hong, H. Zhou, X. Xu, N. De Marco, P. Sun, Z. Zhao, Y.B. Cheng, Y. Yang, Low-temperature TiO_x compact layer for planar heterojunction perovskite solar cells. *ACS Appl Mater Interfaces* 8 (2016) 11076–83.
- [19] F.Cai, J. Cai, L. Yang, W. Li, R.S. Gurney, H. Yi, A. Iraqi, D. Liu, T. Wang, Molecular engineering of conjugated polymers for efficient hole transport and defect passivation in perovskite solar cells, *Nano Energy*,45 (2018)28-36.
- [20] Y. Lin, Z.G. Zhang, H. Bai, Y. Li, X. Zhan, A star-shaped oligothiophene end-capped with alkyl cyanoacetate groups for solution-processed organic solar cells, *Chem. Commun.* 48 (2012) 9655-9657.
- [21] S. Zeng, L. Yin, C. Ji, X. Jiang, K. Li, Y. Li, Y. Wang, D– π –A– π –D type benzothiadiazole–triphenylamine based small molecules containing cyano on the π -bridge for solution-processed organic solar cells with high open-circuit voltage, *Chem. Commun.* 48 (2012) 10627-10629.

- [22] Z. Tan, I. Imae, K. Komaguchi, Y. Ooyama, J. Ohshita and Y. Harima, Effects of π -conjugated side chains on properties and performances of photovoltaic copolymers, *Synth. Met.* 187 (2014) 30-36.
- [23] A. Casey, Y. Han, Z. Fei, A.J. White, T.D. Anthopoulos, M. Heeney, Cyano substituted benzothiadiazole: a novel acceptor inducing n-type behaviour in conjugated polymers, *J. Mater. Chem. C* 3 (2015) 265-275.
- [24] K. Mahesh, S. Karpagam, Synthesis and optoelectronic properties of thiophene donor and thiazole acceptor based blue fluorescent conjugated oligomers, *J. Fluoresce.* 26 (2016) 1457-1466.
- [25] Z.F. Shi, H.T. Black, A. Dadvand, D.F. Perepichka, Pentacenobis (thiadiazole) dione, an n-Type Semiconductor for Field-Effect Transistors, *J. Org. Chem.* 79 (2014) 5858-5860.
- [26] P. Leriche, P. Frere, A. Cravino, O. Alévêque, J. Roncali, Molecular engineering of the internal charge transfer in thiophene– triphenylamine hybrid π -conjugated systems, *J. Org. Chem.* 72 (2007) 8332-8336.
- [27] P. Sonar, E.L. Williams, S.P. Singh, A. Dodabalapur, Thiophene–benzothiadiazole–thiophene (D–A–D) based polymers: effect of donor/acceptor moieties adjacent to D–A–D segment on photophysical and photovoltaic properties, *J. Mater. Chem.* 21 (2011) 10532-10541.
- [28] Z.G. Zhang, Y. Yang, S. Zhang, J. Min, J. Zhang, M. Zhang, Y. Li, Effect of acceptor substituents on photophysical and photovoltaic properties of triphenylamine–carbazole alternating copolymers, *Synth.Met.* 161 (2011) 1383-1389.
- [29] M.S. Liu, X. Jiang, S.Liu, P. Herguth, A.K-Y. Jen, Effect of cyano substituents on electron affinity and electron transporting properties of conjugated polymers, *Macromolecules*, 35 (2002) 3532-3538.
- [30] Z. Gao, Y. Hao, M. Zheng, Y. Chen, A fluorescent dye with large Stokes shift and high stability: synthesis and application to live cell imaging, *RSC Adv.* 7 (2017) 7604-7609.
- [31] S. Selvakumar, K. Sivaji, A.A. Chakkaravarthi, S. Sankar, Enhanced fluorescence and time resolved fluorescence properties of p-terphenyl crystal grown by selective self seeded vertical Bridgman technique, *Mater. Let.* 61 (2007) 4718-21.
- [32] H. Qin, L. Li, Y. Li, X. Peng, J. Peng, Y. Cao, W. Shi, Enhancing the performance of a thieno [3-4-b] pyrazine based polymer solar cell by introducing ethynylene linkages, *Eur. Polym. J.* 48 (2012) 2076-2084.
- [33] X. Zhao, X. Zhan, Electron transporting semiconducting polymers in organic electronics, *Chem. Soc. Rev.* 40 (2011) 3728-3743.
- [34] S.J. Yoon, J.H. Kim, J.W. Chung, S.Y. Park, Exploring the minimal structure of a wholly aromatic organogelator: simply adding two β -cyano groups to distyrylbenzene, *J. Mater. Chem.* 21 (2011) 18971-18973.

- [35] T. Putnin, H. Le, T-T. Bui, J.Jakmune, K. Ounnunkad, S. Peralta, P-H Aubert, F. Goubard, A. Farcas, Poly(3,4-ethylenedioxythiophene/permethylated β -cyclodextrin) polypseudorotaxane and polyrotaxane: Synthesis, characterization and application as hole transporting materials in perovskite solar cells” European Polymer Journal
DOI: 10.1016/j.eurpolymj.2018.06.005
- [36] Y. Guo, C. Liu, K. Inoue, K. Harano, H. Tanaka, E. Nakamura, Enhancement in the efficiency of an organic–inorganic hybrid solar cell with a doped P3HT hole-transporting layer on a void-free perovskite active layer. *J. Mater. Chem. A* 2 (2014) 13827–13830.
- [37] J. H. Heo, S. H. Im, CH₃NH₃PbI₃/poly-3-hexylthiophen perovskite mesoscopic solar cells: Performance enhancement by Li-assisted hole conduction *Phys. Status Solidi RRL* 8, (2014) 816–821.
- [38] N.H. Tiep, Z. Ku, H.J. Fan, Recent Advances in Improving the Stability of Perovskite Solar Cells, *Adv. Energy Mater.* 6 (2015) 1–19.
- [39] T.A. Berhe, W.-N. Su, C.-H. Chen, C.-J. Pan, J.-H. Cheng, H.-M. Chen, M.-C. Tsai, L.-Y. Chen, A.A. Dubale, B.-J. Hwang, Organometal halide perovskite solar cells: degradation and stability, *Energy Environ. Sci.* 9 (2016) 323–356.
- [40] An-Na Cho, Hui-Seon Kim, Thanh-Tuân Bui, Xavier Sallenave, Fabrice Goubard and Nam-Gyu Park Role of LiTFSI in high Tg triphenylamine-based hole transporting material in perovskite solar cell *RSC Adv.* 6 (2016) 68553-68559.